

# Sensing, Control, and In Situ Measurement of Coating Properties: An Integrated Approach Toward Establishing Process-Property Correlations

S. Sampath, V. Srinivasan, A. Valarezo, A. Vaidya, and T. Streibl

(Submitted November 17, 2008; in revised form February 22, 2009)

Over the last decade there has been an explosion in terms of available tools for sensing the particle spray stream in thermal spray processes. This has led to considerable enhancement in our understanding of process reproducibility and reliability. Despite these advances, the linkage to coating properties has continued to be an enigma. This is partially due to the complex nature of the build-up process and the associated issues with measuring properties of these complex coatings. In this paper, we identify critical issues in processing-structure-property relations particularly with respect to the linkage to particle properties. Our goal is to demonstrate an integrated strategy, one that combines particle state sensing, with process mapping and extracting coating properties in situ through the development of robust and advanced curvature-based techniques. These techniques allow estimation of coating modulus, residual stress and, non-linear response of thermal sprayed ceramic coatings all within minutes of the deposition process. Finally, the integrated strategy examines the role of process maps for control of the spray stream as well as tailoring properties of thermal spray coatings. Examples of such studies for yttria-stabilized zirconia thermal barrier coatings are discussed.

**Keywords** CoNiCrAlY, in-flight particle state, in situ coating property measurement, process map, process monitoring and control, TBC, YSZ

## 1. Introduction

In recent years number of robust and user-friendly particle diagnostic tools have become available for thermal spray processes. These have significantly enhanced our ability to monitor the particle state and spray stream in thermal spray processes. Broadly, two techniques of measurement are followed—one based on individual particle measurements and another set based on ensemble (group of particles) measurement. These diagnostics tools allow assessment of in-flight particle temperature, velocity, trajectory, and to a first approximation particle size. Typically, these sensors work on the general principle of two color optical pyrometry and time triggered measurements of velocity. Detailed discussion of these sensors is available in literature—e.g., DPV2000 (Ref 1) for the

single particle-based technique and Inflight Particle Pyrometer, Spray Position Trajectory sensor (Ref 2-4), SprayWatch (Ref 5), and Accuraspray (Ref 6) for ensemble techniques.

As these technologies have matured and become cost effective, there has been a significant increase in their utilization. The principal reason for this is the increasing need to enhance process reliability, reproducibility, and to ultimately meet the goal of producing prime reliant coatings. Although thermal barrier coatings have been the most significant benefactor of these developments, numerous other opportunities exist on the horizon that can benefit from these improvements.

To meet these future goals of reliable/re-producible coating, there are two principal requirements:

1. *Producing reliable and reproducible particle state(s):* The dynamic nature of air plasma spray process introduces variability at different stages in the process to different extents. The particle properties are controlled by torch operation conditions, characteristics of the feedstock material, injection location particularly for external radial injection etc. Other events such as cathode wear, instabilities, etc., can also affect the particle state over time. Operational and time factors also have to be considered to achieve the required particle state in a reliable manner.
2. *Achieve reproducible deposit characteristics:* This not only requires a “reproducible” particle state but also understanding, consideration, and control of other

S. Sampath, V. Srinivasan, A. Valarezo, A. Vaidya, and T. Streibl, Department of Materials Science and Engineering, Center for Thermal Spray Research, Stony Brook University, 130 Heavy Engineering Building, Stony Brook, NY 11794-2275. Contact e-mail: ssampath@ms.cc.sunysb.edu.

factors influencing the coating build-up process. For instance, considerable variability exists in the stochastic splat-based build-up process, which is influenced by deposition conditions such as rate of deposition and angle of impact of particles. Factors such as substrate surface condition and temperature are known to impact the coating characteristics by influencing the adhesion, stress evolution, and other aspects of deposit formation dynamics.

There is considerable activity around the world to address the above two attributes from scientific and engineering standpoint, both numerically and experimentally. The advent of in-flight particle diagnostics, understanding of particle-flame interactions and particle state has allowed assessment of the spray stream conditions and particle state. A variety of efforts over the last few decades have addressed the particle state (Ref 7) and its implication on coating build up (Ref 8). Several reports on successful correlation between particle properties and coating microstructure have been made (Ref 9, 10).

The general consensus to achieving reliable coating characteristics is to understand the different sub-processes, monitor the process, and control the critical variables as necessary within a certain window. Different process sensing and control methodologies have been attempted in order to achieve reliable coating characteristics. Some control the process at the hardware level and some at the in-flight particle level. Studies have suggested that control of particle state is better than simple hardware level control such as controlling total output power (Ref 11, 12). Another recent study has shown particle injection to be vital in achieving reliable particle state and in monitoring them reliably as well as in achieving reproducible coatings (Ref 13, 14). More complex feedback-based real-time control of the process has been attempted using ensemble in-flight process sensor toward achieving the same objective—reliable process and reproducible coatings (Ref 3).

In addition to particle state correlations, several studies have examined the role of substrate temperature and deposition rate effects which can play a significant role not only in deposit formation dynamics but can create new class of thermal barrier microstructures viz segmented cracks or dense vertically cracked microstructure with implications for strain tolerance in thermo-structural coatings (Ref 15-22).

Despite these developments a number of uncertainties remain, which raises the following questions.

- How do single particle and ensemble measurements differ in reporting particle data?
- Is T & V a sufficient descriptor of particle state?
- Does knowledge of particle state provide a sufficient description of ensuing deposit characteristics?
- What are some important coating characteristics one needs to consider for quantitative description?

- Can these characteristics be measured or sensed in situ within the spray booth?

The first three questions will be addressed through some key experimental results presented in this paper using commercial diagnostic instrumentation and the balance will be partly addressed through a recent development (Ref 23-25) at the Center for Thermal Spray Research (CTSR), Stony Brook, through the establishment of in situ coating property sensor (ICP)—a method to extract, during deposition and cooling, residual stresses, elastic modulus of coatings deposited on substrate beams by recourse to measurement of substrate curvature. Although similar approaches have been applied to measure residual stresses (Ref 26), the above method allows for assessment of elastic modulus and non-linear elastic response of thermo-structural ceramic coatings within the confines of the spray booth. Furthermore, the new method uses non-contact, multi-point laser-based sensing (no spectral reflection required) that can operate directly within the confines of a thermal spray booth and the associated harsh environment. Details of the instrument and the associated capabilities and results are provided in Ref 23, 24. Extraction of non-linear properties of ceramic coatings from curvature-temperature data during cooling or post-spray thermal cycling is achieved through a novel analysis procedure discussed in Ref 27, 28.

Finally, at CTSR, an integrated effort is underway to systematically link the phenomena and variability for the various sub-processes during thermal spraying. The ultimate goal is to develop “process maps” which will provide a scientific framework for coating design and to assess parametric effects and variability.

## 2. Experimental Details

### 2.1 Materials and Process

In this investigation one of the most commonly used TBC system materials—yttria-stabilized zirconia (YSZ)—has been studied using plasma spray process. In addition, comparative experiments have been conducted on the bond coat material CoNiCrAlY with both plasma and HVOF processes. Both materials have been studied in terms of particle state but the top coat YSZ has been studied in more detail with respect to coating characteristics and process reliability. Multiple hardware configurations have been examined and results are presented here predominantly for an external injection Sulzer Metco 7 MB torch operated with N<sub>2</sub>-H<sub>2</sub> parameters. Tables 1 and 2 list some of the key spray parameters used in this study. Parameters not mentioned in the tables have not been varied unless mentioned specifically. Process parameters were based on a more rigorous experimental design-based process map approach which is described in Ref 29.

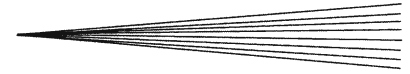


**Table 1 Typical plasma spray parameters used for the various experiments discussed in the paper**

Experiment	Powder	Primary gas flow, slpm	Secondary gas flow, slpm	Current, A	Voltage, V	Carrier gas flow, slpm	Spray distance, mm	Torch & gases	Results in section
Comparison of single particle and ensemble sensors	CoNiCrAlY—Praxair CO-211 YSZ—St. Gobain HW1532	38-57	3-9	500-600	65.6-75.5	3.7-5.4	130	SM 7 MB/N <sub>2</sub> -H <sub>2</sub>	3.1
Implications of distributions	YSZ—St. Gobain HW1532	48	5.6	550	72	4.8	130	SM 7 MB/N <sub>2</sub> -H <sub>2</sub>	3.2
Is T & V a sufficient descriptor of particle state?	YSZ—Sulzer Metco AE7592	39	21	850	39	4.5	60-120	SG 100/Ar-He	3.3.1
Process control based on average particle T & V	YSZ—Sulzer Metco 204NS	41-53	1.7-12.0	434-706	68.7-83.5	4.0-4.6	130	SM 7 MB/N <sub>2</sub> -H <sub>2</sub>	3.3.2
Is T & V a sufficient descriptor of ensuing deposit characteristics	YSZ—Sulzer Metco AE7592, AE7593, AE7216	40	10	650	66-68	3	100	SM F4/Ar-H <sub>2</sub>	3.3.3
	YSZ—Sulzer Metco 204NS, St. Gobain HW 1532, H.C. Starck 832.090	48-52	6.9-7.1	466-548	76.6-80.0	4.2-6.0	130	SM 7 MB/N <sub>2</sub> -H <sub>2</sub>	
In situ measurement of non-linear elastic response of ceramic coatings	YSZ—St. Gobain HW 1532, St. Gobain HW 1622, H.C. Starck 832.090	48-52	5.6-7.1	466-550	76.6-80.0	4.2-6.0	130	SM 7 MB/N <sub>2</sub> -H <sub>2</sub>	3.4

**Table 2** Typical plasma spray parameters used for the various experiments discussed in the paper

Experiment	Powder	Torch & gases	Fuel, slpm	Oxygen, slpm	Air, slpm	Carrier flow, slpm	Spray distance, mm	Feed rate, g/min	Results in section
Particle state and deposit residual stress	CoNiCrAlY— Praxair CO-211-1	HVOF-DJ/SM	60/C <sub>3</sub> H <sub>6</sub>	197	350	12/N <sub>2</sub>	266	30	3.5
		HVOF-JK/Stellite	540/H <sub>2</sub>	190	...	31/Ar	225	30	
		HVOF-JP-5000/Praxair	0.322/Kerosene	897	...	4.7/Ar	266	90	

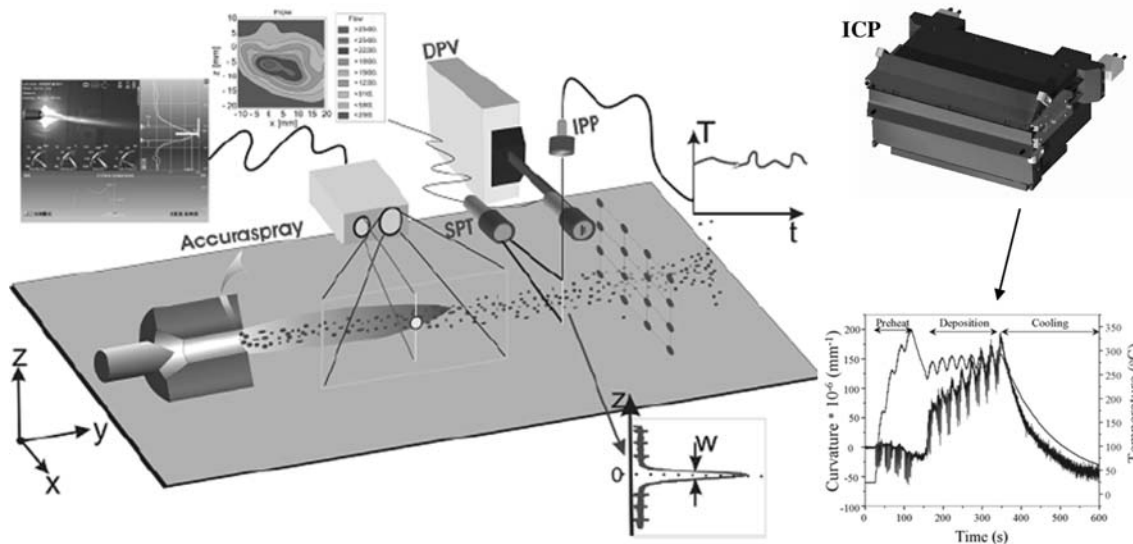


**Fig. 1** Illustration of integrated 3D diagnostic setup and the in situ coating property sensor ICP. The 3D sensor setup comprises of DPV 2000, Accuraspray (both from Tecnar Automation, Quebec) as well as the spray position trajectory (SPT) and inflight particle pyrometer (IPP) both from Inflight Inc., Idaho Falls, ID

Commercially available YSZ powders were examined in this study. Both plasma densified hollow sphere (PD) feedstock (Sulzer Metco 204NS), a fused and crushed (FC) materials (St. Gobain Ceramics) and an agglomerated and sintered powder (from HC Starck Inc.) were examined. The materials were commercially available feedstock as standard products. The particle size distribution followed a Gaussian distribution in the broad range of 10–70  $\mu\text{m}$ . In one study, two size distributions were obtained by sieving the commercially available FC material. The size distributions of the two cuts ranged from 5 to 45  $\mu\text{m}$  and the other from 45 to 70  $\mu\text{m}$ . The CoNiCrAlY material was also a commonly available commercial material produced via gas atomization with size distribution of 10–53  $\mu\text{m}$  obtained as a specialty item from Praxair Inc, Indianapolis.

The three significant torch parameters, namely primary gas flow, secondary gas flow, and current, have been varied systematically via a design of experiment (DoE) and the data from different sensors are compared in this study for both materials (for more information refer Ref 29). Past work has shown that particle injection is a critical step particularly for orthogonal external injection of low density particles such as zirconia as particle sometimes do not penetrate the spray plume. It is generally appreciated that there exists an optimum injection location at which

maximum energy transfer between plasma and particle occurs. When particle states resulting from different torch parameters are compared, it is important that the comparison be made from measurements at the optimum injection condition for each torch parameter combination in order to reveal the real influence of torch parameters. In this investigation, particle injection was optimized for each process condition considered by controlling the trajectory (angle of the spray stream) using data from spray position trajectory (SPT) sensors. Details of the phenomena and procedures are reported elsewhere (Ref 13).

## 2.2 Sensor Setup and Measurements

To achieve a map of the spray stream, a suite of diagnostic sensors have been arranged in a 3D setup as shown in Fig. 1. This 3D strategy is particularly important for swirl flow plasma torches and spraying of relatively light powder materials such as zirconia. It has been observed that particles do not always follow an axial flow path but can experience a rotational component which can affect both sensor measurement and deposition. Detailed description of sensors and the procedure followed has been discussed in various references (Ref 13, 29, 30).

Deposits are produced on grit-blasted aluminum beams mounted on a specially devised in situ curvature sensor

(Ref 23, 24). Aluminum was chosen as a substrate for a number of reasons. First, it exhibits a larger curvature in the sample due to larger mismatch during the low-temperature cycling. The relative CTE mismatch between the YSZ and aluminum at the temperature range of cycling (ambient to 250 °C) mimics the mismatch between the YSZ and superalloy in the actual operating temperature range (ambient to >1000 °C). Finally, the native oxide in the aluminum is more akin to those found in traditional bond coats compared to steel. During deposition (pre-heating, coating, and cooling), the curvature evolution and substrate temperature are monitored. Subsequent to deposition, the coated bi-material beam is thermally cycled with a hand torch by gently heating to about 250 °C. The process takes a few seconds and system is allowed to stabilize followed by a relatively longer cooling down period (~20 min). During this period, the curvature evolution and substrate temperature are monitored. The system is nominally isothermal at the end of the heat cycle and allowed to cool down slowly. By examining curvature-temperature results (during cooling) and through recourse to detailed non-linear bi-material beam solution, it is possible to extract the non-linear elastic stress-strain properties of the spray deposited ceramic coatings (Ref 28, 31). The non-linearity is introduced by the porous nature and numerous interfacial gaps in the coating. Through interpretation of the results it is possible to interpret the linkages to particle state and other deposition parameters (Ref 32).

Finally, the coating density/porosity, microstructure and thermal conductivity are measured by removing the substrate and measuring the properties of the freestanding forms. Again, linkages to the process attributes can be established (Ref 33, 34).

### 3. Results and Discussion

#### 3.1 Comparison of Single Particle and Ensemble (Group) Measurements

The basic principles of measurement of in-flight particle data, namely temperature and velocity, are the same

for the in-flight diagnostic sensors, single particle and ensemble (at least in the case of the sensors considered in this study). The key difference in reported data is due to differences in measurement volume, time of integration of data (number of particles), and the ability to scan the spray stream. These parameters determine if the data are from a single particle or from multiple particles, how representative the data is to the spray stream/process and the reliability and accuracy of the data.

Among the various in-flight process monitoring sensors, DPV 2000 has been a workhorse R&D tool with its capability to measure individual particle temperature, velocity, and size. Other sensors such as Accuraspray provide information for an ensemble of particles. The integrated diagnostic setup as shown in Fig. 1 allows cross-comparison of single and ensemble particle-based measurement during the same or similar time domain. Such studies were conducted for the widely used TBC materials YSZ (Fig. 2) and CoNiCrAlY (Fig. 3). The data presented here compare only DPV and Accuraspray data as they both work on identical principles and manufactured by the same company.

It is important to note that the specific location of measurement among the two sensors is critical for effective comparison. Two factors made appropriate comparison possible in this study. First is the 3D sensor setup with precisely known coordinates, corresponding robot manipulation and measurements with sensors at the same location in the spray stream (Ref 30). Second, optimized particle injection through the use of SPT sensor (Ref 13) which not only results in optimized particle state for each of the different process parameters but also maintains the same particle trajectory ensuring reliable measurement of the particle data at the same location in the spray stream. This is a key step especially when process sensors are measuring along an axis mutually perpendicular to the spray axis and the axis of injection. Benefits of this approach are more elaborately described in Ref 13, 14.

Average particle velocity from single particle sensor (obtained from approximately 10,000 particles) and ensemble sensor (single group measurement) shows good correlation for both YSZ ceramic and CoNiCrAlY

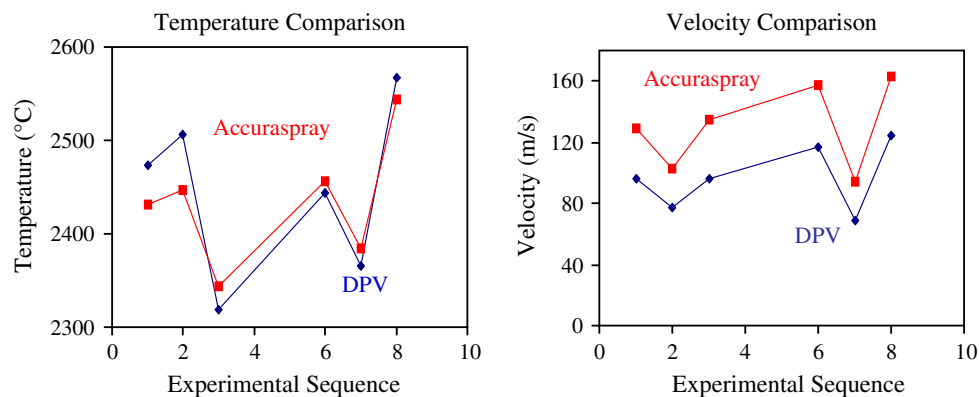


**Fig. 2** Comparison between DPV and Accuraspray for YSZ: particle temperature (left) and particle velocity (right)

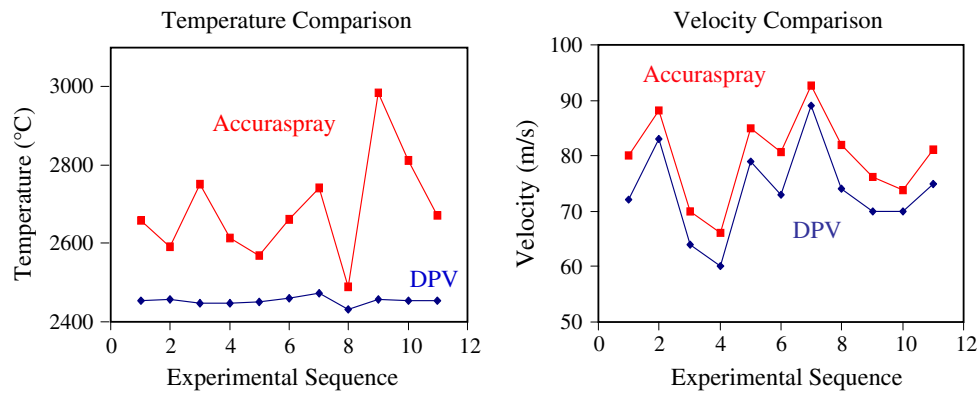


**Fig. 3** Comparison between DPV and Accuraspray for CoNiCrAlY: particle temperature (left) and particle velocity (right)

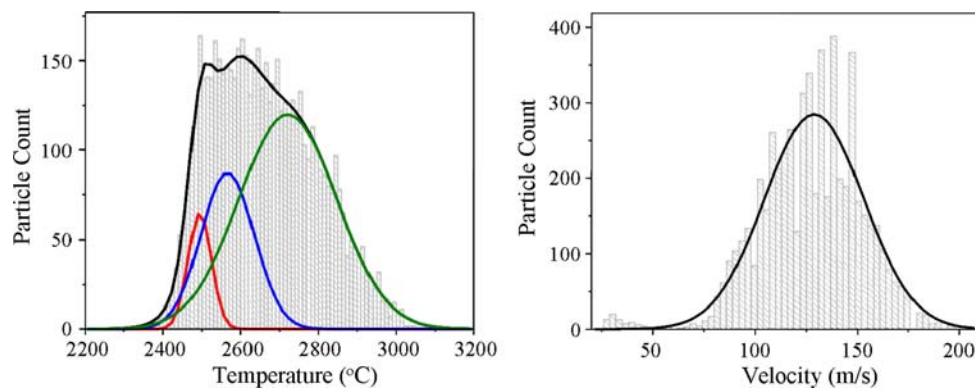


**Fig. 4** Typical distribution of particle temperature and velocity for YSZ. While the velocity distribution is observed to be Gaussian, the temperature distribution is multimodal and not Gaussian

metallic material systems for a range of operating conditions. Average particle temperature from single particle and ensemble sensor shows good correlation for YSZ but not for CoNiCrAlY. The results suggest that for high-temperature materials such as YSZ (higher total radiated intensity due to higher temperature and higher emissivity), the two types of sensors can be cross-correlated at least when investigated in a controlled environment such as a laboratory. However, the results also point to the need for additional studies in the case of metals/alloys or lower temperature materials to understand the fundamental characteristics of these diagnostic tools and their data output. Issues related to oxidation and change of emissivity need concurrent consideration.

### 3.2 Implications of Distributions

Typically, data from ensemble sensors are reported as an average number representative of the measurement volume of the sensor while the data from single particle sensor are location-specific (in the spray stream) and can be represented as distributions as shown in Fig. 4. The distribution of particle velocity in general follows a normal (Gaussian) distribution, while the particle temperature

displays a multimodal behavior. This raises concern whether mean and standard deviation are appropriate indicators to represent the data from a simple statistical standpoint. Previous work has shown that a critical analysis of this multimodal distribution indicates the presence of a nominal melting threshold represented by the first peak of the distribution. The position of this peak was found to be invariant across a spectrum of operating conditions, suggesting the centroid of the peak to represent the nominal melting point of the particular material: in this case YSZ (Ref 30). [The melting peak is at a constant temperature (for a given calibration setting of the pyrometric detector) and is independent of particle size, powder morphology, and process parameters.] Details of this analysis are provided elsewhere (Ref 30) but it is important to note that these multimodal peaks can skew the reported averages in particle temperatures for a given spray condition.

The ensemble measurements, on the other hand, cannot provide information on the melting state of the particles but simply provide a “characteristic value” involving both molten and unmolten particles. Thus, one can conclude that caution is warranted in linking sensor reported temperature results with description of the entire particle behavior and ensuing properties.

### 3.3 Relationship Between Particle State and Deposit Evolution

Here we discuss the significance of particle state on deposit evolution and properties.

**3.3.1 Is T & V a Sufficient Descriptor of Particle State?** In the previous section, we discussed the insufficiency of measured particle temperature in describing the molten status of the spray particle, particularly those of the ceramics. However, various past studies have suggested that average temperature and velocity to a first approximation control the microstructure and properties of coatings. In fact, this has been the basis of widespread implementation of particle state sensors in industrial practice.

In most cases, sensor-based measurements of particle temperatures are usually carried out at the nominal spray distance. Clearly, melting state is not only dependent on the temperature of the radiating particle but also on the temperature history (dwell time) and the particle size. As such it is important to consider temperature, velocity, and size as a grouped variable in describing the effects of particle state on deposit formation. Earlier work by Vaidya et al. (Ref 35) has shown that the melting state of ceramic particles can be described through group parameter referred to as melting index. In its simplest form, the melting index is the measured particle temperature normalized with respect to size and velocity and therefore provides a framework to incorporate both material volume and dwell time. This is expressed as:

$$MI = \frac{T\Delta t_{fly}}{D} \quad (\text{Eq 1})$$

where  $T$  is the measured particle surface temperature (K),  $D$  is the particle size (m), and  $\Delta t_{fly}$  is the particle in-flight time assuming constant acceleration of particles (s), which has the following expression:

$$\Delta t_{fly} = \frac{2L}{V} \quad (\text{Eq 2})$$

where  $L$  is the spray distance (m) and  $V$  is the particle velocity (m/s). More comprehensive formulations have also been derived by Zhang et al. (Ref 36) and made non-dimensional. Melting index can be readily extracted from DPV 2000 experimental data as it measures individual

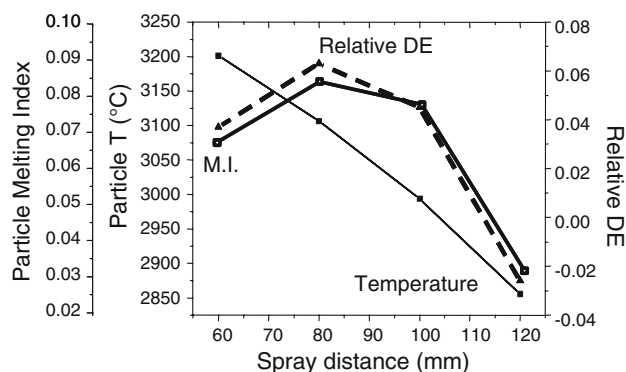


**Fig. 5** Relationship between particle temperature and melting index on the relative deposition efficiency (DE) (Ref 37)

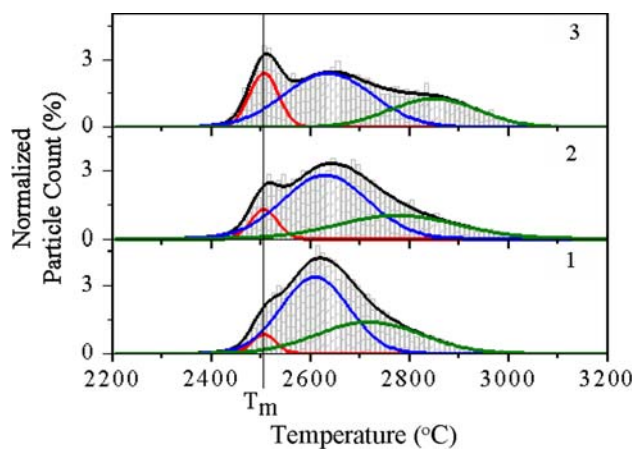
particle temperature, velocity, and size. Such measurements and analysis have been conducted for a large range of plasma spray materials and have been discussed in a recent publication (Ref 37).

The implication of selecting group parameters rather than particle temperature alone to describe particle state effects on deposition efficiency is shown in Fig. 5. Here, the results indicate that despite a monotonic decrease in particle temperature with spray distance the relative deposition efficiency actually increases initially and then decreases. In contrast, the melting index of the particle does not follow such a monotonic behavior. The correlation of deposition rate (relative deposition efficiency) to melting index seems much more appropriate than particle temperature in the case of varying spray distance. This suggests that at least for YSZ temperature alone is perhaps not a complete descriptor of melting state (Ref 38).

### 3.3.2 Process Monitoring and Feedback Control Based on Average Particle Temperature and Velocity.

Since temperature and velocity of the particles are directly measured in the spray booth, it is worth considering them as the important output variables for feedback control of the plasma spray process to account for variability in the spray process with respect to process parameters. In this study, a few controlled experiments were performed by precisely controlling the particle state to be within a small window of  $\pm 10^\circ\text{C}$  average particle temperature and  $\pm 2$  m/s average particle velocity using widely varying the plasma-forming torch parameters ( $\text{N}_2$ ,  $\text{H}_2$ , and current) for the same feedstock powder. At each combination of torch parameters,  $\text{H}_2$  flow was fixed and  $\text{N}_2$  flow and current were adjusted guided by torch parameter vectors in T-V space to result in same average T & V. The torch parameter vectors in T-V space were established based on first order process map (equations established between torch parameters and particle state) (Ref 29).

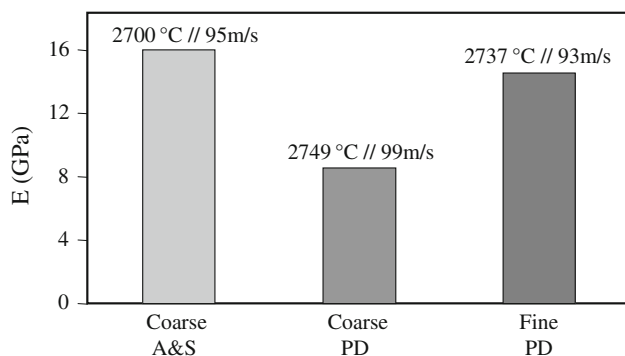
Particle temperature distributions from the different spray conditions which nominally yield the same average temperature in the DPV data are shown in Fig. 6 and



**Fig. 6** Particle temperature distribution from three experiments (extremes and intermediate) that resulted in comparable average temperatures and velocities (within a small window of  $\pm 10^\circ\text{C}$  and  $\pm 2$  m/s)

**Table 3 Detailed characterization of particle states and coating properties for YSZ conditions reported in Fig. 6**

Spray condition	Average temperature, °C	Average velocity, m/s	Melting index	Reynolds number	Ensemble temperature, °C	Relative DE	Thermal conductivity, W/mK	Indentation modulus, GPa	Curvature modulus, GPa
1	2644	123	0.017	649	2499	100	1.03 ± 0.09	31.1 ± 1.1	23.6
2	2666	125	0.019	718	2730	93	1.12 ± 0.03	33.9 ± 1.2	25.6
3	2672	125	0.021	679	2877	72	0.91 ± 0.01	30.1 ± 1.3	27.1

**Fig. 7** In-plane elastic modulus of coatings obtained from in situ curvature measurements for three different powders nominally reflecting similar particle state

other properties are shown in Table 3. It is clear that the distributions are multimodal and significantly different despite reporting the same average. The distribution resulting from condition 1 (shown in the bottom figure) is indicative of better melting than the one at the top figure (condition 3) as most of the distribution lie to right of the nominal melting peak. Condition 2 represents an intermediate condition. For these three conditions, the ensemble measurements of temperatures are notably different as is the average melting index of the spray stream. Furthermore, differences of about 30% could be observed in deposition efficiency and through thickness indentation modulus between these coatings. In the case of DPV, it is possible to interpret the melting peak but similar assessment is difficult for ensemble measurements. As such it is clear that careful consideration of both sensor reported data and parameter selection is required in terms of feedback control.

**3.3.3 Is T & V a Sufficient Descriptor of Ensuing Deposit Characteristics?** Past studies have shown correlations between particle state and deposit microstructures (usually porosity). Through the use of the in situ curvature system (Ref 23, 24), it has been possible to extract the residual stress evolution and the elastic modulus of the sprayed layer. Figure 7 shows the results for three sets of YSZ powders: two of the same morphology of different sizes (PD) and also a comparison of two morphologies [PD and A&S (agglomerated and sintered)] of the same size distribution. The particle diagnostics results of the three powders for the operated conditions yielded temperature and velocity results that were nominally in the same range (within a few percent

as shown in Fig. 7). However, the in-plane elastic modulus results indicate substantial differences among the coatings.

In another series of experiments, three different feedstock morphologies of comparable particle sizes were processed under tightly controlled particle state conditions ( $\pm 10$  °C and  $\pm 2$  m/s) achieved under similar secondary gas flow rates [a robust feedback control strategy was applied here (Ref 29)]. The results shown in Fig. 8 indicate that the thickness per pass (considered here as a parameter to describe deposit evolution and process efficiency) is different for different morphologies despite the particles displaying similar average T & V. The plasma densified (PD) powder which comprises of particles with hollow sphere morphology shows a higher thickness per pass as a result of increased deposit efficiency compared to the fused and crushed (FC) powder and the agglomerated and sintered (AS) material. This is despite the particle having a smaller mass for equivalent volume. Furthermore, the in-plane modulus from the in situ sensor and the through thickness thermal conductivity are also substantially different among the three coatings. This confirms the results on microstructural differences of YSZ coatings prepared from different morphologies (Ref 39-42). Again, these results suggest that discretion is required in using purely T & V as a guide to predicting ensuing coating properties.

With due consideration of the above-mentioned issues and through careful integration of the process parameter selection, particle state sensing, and property extraction (via the framework of process maps), it is feasible to extract the linkage between particle state and resulting coating properties (Ref 19, 29, 43). However, additional attributes such as substrate conditions (temperature, roughness), deposition conditions (rate, spray angle) will all contribute to the deposit characteristics by influencing wetting, spreading-splashing, flattening, solidification, and interlocking/bonding dynamics. Therefore, a full description of the deposit state will require these additional parameters to be considered. Such studies have been conducted for plasma sprayed Mo, YSZ, and TiO<sub>2</sub> (Ref 19, 29, 43).

### 3.4 In Situ Measurement of Non-Linear Elastic Response of Ceramic Coatings

The complex defected nature of thermal sprayed ceramic coatings makes it difficult to fully characterize the mechanical behavior of these materials. For instance, plasma sprayed YSZ coatings typically yield elastic



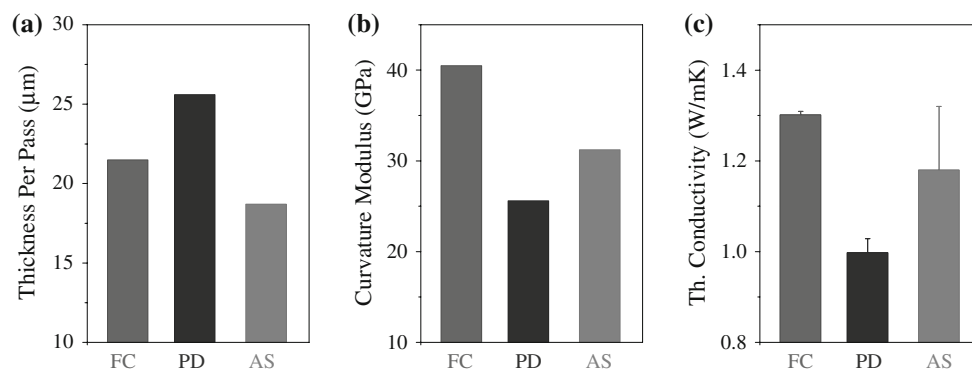


**Fig. 8** Properties of coatings processed using three different powder morphologies at nominally the same average temperatures and velocities (within a small window of  $\pm 10$  °C and  $\pm 2$  m/s)

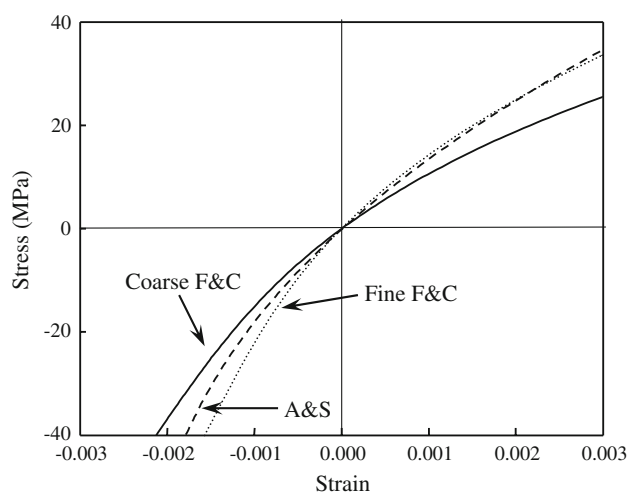


**Fig. 9** Non-linear elastic stress-strain relationships obtained from in situ curvature measurements

modulus and thermal conductivity that are about 20-30% of theoretical value and generally cannot be described by the total porosity alone. Over the years there have been several anecdotal results which have indicated that thermal sprayed ceramic coatings display a non-linear elastic behavior.

Recent investigations using the in situ curvature sensor and through recourse to post-spray thermal cycling have shown the curvature-temperature relationship to be non-linear and perhaps even *anelastic* (i.e., a hysteresis in the loading/unloading curve associated with energy dissipation mechanisms). Detailed report on these findings is discussed elsewhere (Ref 28, 31), but we present here one example of the result as extracted from the integrated sensor strategy. Figure 9 shows the stress-strain relationship for YSZ coatings of two morphologies and two size distributions which is similar to those described in Fig. 8.

These results have important implications on the design and performance of plasma sprayed ceramics notably

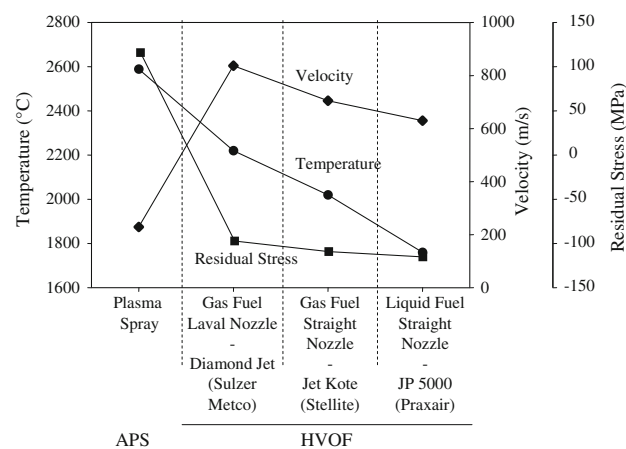


**Fig. 10** Relationships among particle state and deposit residual stresses for APS and HVOF deposited CoNiCrAlY coatings. The differences in the HVOF arise from nozzle shapes and type of fuel used

thermal barrier coatings as they provide insight into the response of these defected microstructures on the thermo-mechanical performance of coatings. Of particular importance is that it is now possible to extract these design-relevant information and be able to do so in situ within the confines of the thermal spray booth. Coupled with the capability to tune the particle state, and other process variables, it is feasible to introduce controlled elastic properties with implications for thermo-mechanical compliance.

### 3.5 Extending the Linkages Across Processes: APS and HVOF CoNiCrAlY Coatings

The particle properties to a first approximation also can be linked to coating residual stresses especially for metallic coatings. Figure 10 displays the results of particle properties comparing APS with various types of HVOF processes and nozzle geometries. The particle temperature in Fig. 10 follows a monotonically lower behavior from left to right

while the particle velocity among the HVOF processes is a function of the nozzle shape. The residual stresses in the coatings are a strong function of the particle velocity and only to a limited extent on particle temperatures. Note that the reported stress here is the final stress which can be a result of different pathways and combinations of the component stresses. For instance, the residual stresses in the metallic APS coating are largely dominated by quenching effects and as such highly tensile while in the case of the HVOF coatings, the stresses resulting from peening effect that dominates over the quenching stresses. In all cases, the thermal mismatch contraction added relatively small tensile stresses due to small CTE mismatch between the coating material and the substrate material (steel) (CTE CoNiCrAlY:  $13.3 \times 10^{-6} \text{ }^\circ\text{C}^{-1}$  and steel AISI 1018:  $11.9 \times 10^{-6} \text{ }^\circ\text{C}^{-1}$ ). Substrate temperature ranged between 120 and 250  $^\circ\text{C}$  for all the experiments. These results point to the requirement of mechanism-driven interpretation of the process-microstructure-property relationships for thermal sprayed materials.

### 3.6 Integrating Sensing with Properties: Synthesis of Process Maps

In the previous section, we have shown the developments and issues relative to the various sub-stages of a typical thermal spray processes including particle state sensing, parametric effects, and measurement of both

traditional and novel properties of coatings. Due to the fact that all of these process sub-stages are interlinked, it is critical to link the parametric effects across the spectrum of measurement. One means to achieve this is through the integrated strategy of process maps. Process maps are interrelationships among the process variables and output responses. In the case of thermal spray they can be divided into two subsets. The relationship between torch parameters and spray stream measured by diagnostics is a direct linkage and can thus be expressed as a first order process map. The relationship between the spray stream measured responses and coating properties is translational step and can be expressed more as a second order process map. Creating a first order and second order map for a given material/thermal spray process will allow systematic evaluation of the processes, ultimately leading to optimization of coating properties for specified performance and/or full field assessment of process reliability. The concept of process maps is illustratively described in earlier work (Ref 19, 29, 43), but is summarized in a simplified manner in Fig. 11.

Concurrent with the flow chart describing process map concept in Fig. 11, quantitative results of the process-particle state linkages are presented in the form of a first order for air plasma spraying YSZ. In this rendition, a T-V diagram is synthesized for a range of torch conditions for a given feedstock material (fused and crushed YSZ). A full factorial central composite design was used to explore the

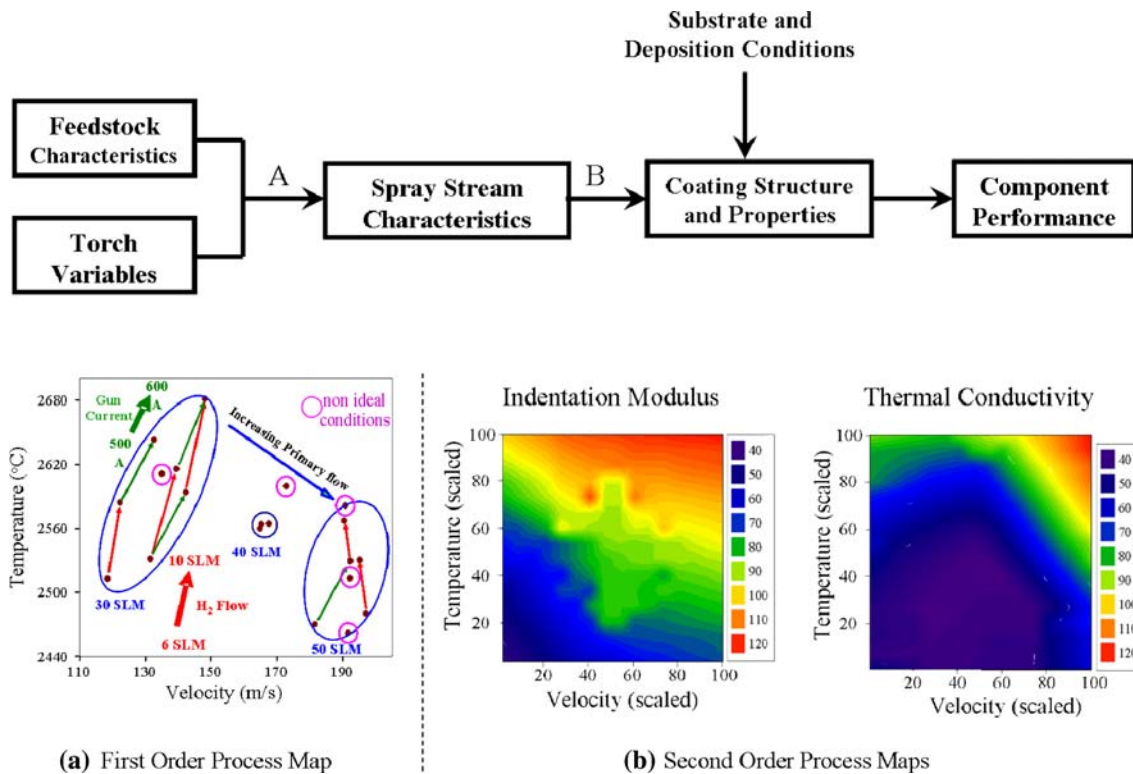


**Fig. 11** Schematic representation of the process map concept enabling a systematic approach to process development as well as the reverse route, i.e. using desired coating properties and seeking process parameters. The first order map also shows strategies for assessing spray stream variability through torch state and other stochastic effects

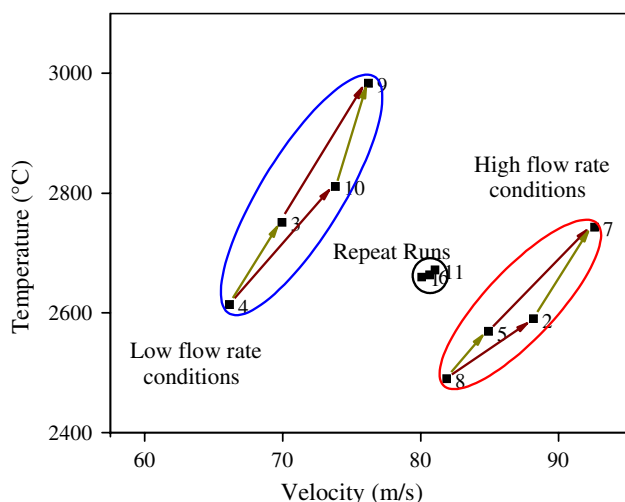


**Fig. 12** First order process map for APS of CoNiCrAlY material. The results here identify the particle state response for various torch operating conditions as well as the control vectors identifying the influence of gun current and secondary gas flow. These vectors are quantitative and can be used for feedback control and synthesis of first order maps with coating property considerations

operational range. These maps are very useful to guide in parameter development, track instabilities, and examine reproducibility. The first order process map shown in Fig. 11(a) indicates how each individual process parameter affects the measured outcomes in terms of particle temperature and particle velocity. Increasing primary gas flow shifts the T-V diagram from left to right and top to down (i.e., higher flows reduce particle temperature and increase particle velocity, which is to be anticipated). Both gun current and secondary gas flow increase the temperatures of the particle but at different levels. Finally, the first order map can also be used to identify instabilities. For instance, the circled points in the first order process map of YSZ highlighted as non-ideal conditions are a result of observed variations from expected output for those specific conditions. Over the years such first order maps have been established for a range of materials, but most notably for YSZ, due to its present day importance (Ref 37). These first order maps also allow for establishment of control vectors for feedback strategies. The results of these approaches have been presented in earlier papers (Ref 14, 30).

However, to utilize such maps from a true coating design perspective, it is important to establish the linkage between particle state space and the coating microstructure/properties. Figure 11 also shows the results of coating elastic modulus and coating thermal conductivity which have been overlaid on the first order map. Such second order maps not only provide visual tools for understanding coating formation dynamics but also schemes for optimization and reliability assessment. Alternative strategies in terms of second order maps can also be considered, for example, microstructure-thermal conductivity or non-linearity-modulus diagrams. Such

results have been presented in earlier papers and can potentially be considered as third order maps. The advantage of developing maps based on these orders is that it allows a systematic exploitation of the entire thermal spray process. Such maps hold the promise for incorporating design criteria upfront in the process development cycle.

The process map concept can also be extended to metallic alloy systems as well as across a range of processes. In Fig. 12, a first order process map for CoNiCrAlY is presented. Despite the fact that CoNiCrAlY material will oxidize in flight, the overall first order map appears very similar. As the plasma gas flow rate is increased, the T-V response shifts to the right and lower in temperature as expected. Within each of the constant primary gas flow rate ellipses (points 4, 3, 9, 10 in low primary gas regime and points 8, 5, 7, 2 in high primary flow regime), the vectors display the effect of increasing hydrogen and gun current. Finally, the repeated center condition illustrates the reliability of the process and the measurements. Such first order maps can be produced rather quickly compared to more elaborate process development schemes and as such provide a mechanism for the controlled development of process-microstructure-property relationships.

#### 4. Summary and Conclusions

This paper summarizes ongoing studies in developing an integrated understanding of thermal spray processes through the use of both particle sensors and coating property assessments. This paper is a synopsis of extensive multiyear investigative strategy and exemplifies important findings. Important conclusions drawn from these studies are listed next.

- Particle sensors are useful for defining the spray stream and provide mechanisms to investigate the role of torch and feedstock parameters on the particle state.
- Radial injection plasma spray generally results in 3D phenomena in terms of particle movement in plume and as such diagnostics needs to be considered and implemented with appropriate care. The integrated setup such as the ones shown in Fig. 1 shed light into not only the process but also cross-correlating various sensors and methodologies.
- Representation of the particle state within the T-V space allows a systematic recognition of the contribution of the process variables and sensitivities. They also provide a framework for feedback control strategies.
- To a first approximation, particle velocity measured from single and ensemble sensors can be correlated but careful consideration is required for understanding the temperature results.
- Particle temperature may not be a sufficient descriptor of the melting state for refractory ceramics and

normalized/group parameters are perhaps more appropriate. Parameters such as melting index, kinetic energy, particle Reynolds number may offer more insights into the description of process states.

- Particle state is important but may not fully describe the evolving deposit state.
- Although elastic modulus is a reasonable quantitative descriptor of a coating property, non-linear response would also have to be considered for porous coatings, especially those subjected to thermo-mechanical loading.
- Particle velocity and temperature can affect residual stress evolution in metallic coatings but require consideration of the underlying mechanisms and contributions of component stresses.
- Integrated process maps provide a framework comprehending sensors, enable feedback control and when combined with coating properties offer a strategy for coating design.

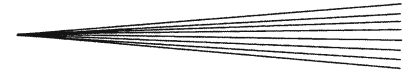
Studies along these lines for various materials and processes have been conducted and are reported in detail in the literature with further enhancements underway.

## Acknowledgments

This work was supported by the GOALI-FRG program of National Science Foundation under award CMMI 0605704. Support through the Stony Brook Industrial Consortium for Thermal Spray Technology is also acknowledged.

## References

1. C. Moreau, P. Gougeon, M. Lamontagne, V. Lacasse, G. Vaudreuil, and P. Cielo, On-Line Control of the Plasma Spraying Process by Monitoring the Temperature, Velocity and Trajectory of In-Flight Particles, *Thermal Spray Industrial Applications: Proceedings of 7th National Thermal Spray Conference* (Boston, MA), ASM International, 1994
2. J.R. Fincke, D.C. Haggard, and W.D. Swank, Particle Temperature Measurement in the Thermal Spray Process, *J. Therm. Spray Technol.*, 2001, **10**(2), p 255-266
3. J.R. Fincke, W.D. Swank, R.L. Bewley, D.C. Haggard, M. Gevelber, and D. Wroblewski, Diagnostics and Control in the Thermal Spray Process, *Surf. Coat. Technol.*, 2001, **146**, p 537-543
4. W.D. Swank, J.R. Fincke, and D.C. Haggard, A Particle Temperature Sensor for Monitoring and Control of the Thermal Spray Process, *Thermal Spray Science and Technology: Proceedings of the 8th National Thermal Spray Conference* (Houston, TX), ASM International, 1995
5. J. Vattulainen, E. Hamalainen, R. Hernberg, P. Vuoristo, and T. Mantyla, Novel Method for In-Flight Particle Temperature and Velocity Measurements in Plasma Spraying Using a Single CCD Camera, *J. Therm. Spray Technol.*, 2001, **10**(1), p 94-104
6. B.R. Marple, J. Voyer, J.F. Bisson, and C. Moreau, Thermal Spraying of Nanostructured Cermet Coatings, *J. Mater. Process. Technol.*, 2001, **117**(3), p 418-423
7. H. Zhang, H.B. Xiong, L.L. Zheng, A. Vaidya, L. Li, and S. Sampath, Melting Behavior of In-Flight Particles and its Effects on Splat Morphology in Plasma Spraying, *International Mechanical Engineering Congress and Exposition* (New Orleans, LA), ASM International, 2002
8. L. Li, X.Y. Wang, G. Wei, A. Vaidya, H. Zhang, and S. Sampath, Substrate Melting During Thermal Spray Splat Quenching, *Thin Solid Films*, 2004, **468**(1-2), p 113-119
9. M. Friis, C. Persson, and J. Wigren, Influence of Particle In-Flight Characteristics on the Microstructure of Atmospheric Plasma Sprayed Yttria Stabilized ZrO<sub>2</sub>, *Surf. Coat. Technol.*, 2001, **141**(2-3), p 115-127
10. M. Prystay, P. Gougeon, and C. Moreau, Structure of Plasma-Sprayed Zirconia Coatings Tailored by Controlling the Temperature and Velocity of the Sprayed Particles, *J. Therm. Spray Technol.*, 2001, **10**(1), p 67-75
11. C. Moreau and L. Leblanc, Optimization and Process Control for High Performance Thermal Spray Coatings, *Durable Surf.*, 2001, **197**, p 27-57
12. J.F. Bisson, C. Moreau, M. Dorfman, C. Dambra, and J. Mallon, Influence of Hydrogen on the Microstructure of Plasma-Sprayed Yttria-Stabilized Zirconia Coatings, *J. Therm. Spray Technol.*, 2005, **14**(1), p 85-90
13. V. Srinivasan, M. Friis, A. Vaidya, T. Streibl, and S. Sampath, Particle Injection in Direct Current Air Plasma Spray: Salient Observations and Optimization Strategies, *Plasma. Chem. Plasma Process.*, 2007, **27**(5), p 609-623
14. V. Srinivasan, A. Vaidya, T. Streibt, M. Friis, and S. Sampath, On the Reproducibility of Air Plasma Spray Process and Control of Particle State, *J. Therm. Spray Technol.*, 2006, **15**(4), p 739-743
15. X. Jiang, J. Matejcek, and S. Sampath, Substrate Temperature Effects on the Splat Formation, Microstructure Development and Properties of Plasma Sprayed Coatings Part II: Case Study for Molybdenum, *Mater. Sci. Eng. A*, 1999, **272**(1), p 189-198
16. X.Y. Jiang, Y.P. Wan, H. Herman, and S. Sampath, Role of Condensates and Adsorbates on Substrate Surface on Fragmentation of Impinging Molten Droplets During Thermal Spray, *Thin Solid Films*, 2001, **385**(1-2), p 132-141
17. R.A. Miller and C.C. Berndt, Performance of Thermal Barrier Coatings in High Heat Flux Environments, *Thin Solid Films*, 1984, **119**(2), p 195-202
18. S. Sampath and X. Jiang, Splat Formation and Microstructure Development During Plasma Spraying: Deposition Temperature Effects, *Mater. Sci. Eng. A*, 2001, **304**, p 144-150
19. S. Sampath, X. Jiang, A. Kulkarni, J. Matejcek, D.L. Gilmore, and R.A. Neiser, Development of Process Maps for Plasma Spray: Case Study for Molybdenum, *Mater. Sci. Eng. A*, 2003, **348**(1-2), p 54-66
20. S. Sampath, X.Y. Jiang, J. Matejcek, A.C. Leger, and A. Vardelle, Substrate Temperature Effects on Splat Formation, Microstructure Development and Properties of Plasma Sprayed Coatings Part I: Case Study for Partially Stabilized Zirconia, *Mater. Sci. Eng. A*, 1999, **272**(1), p 181-188
21. A. Tricoire, A. Vardelle, P. Fauchais, F. Braillard, A. Malie, and P. Bengtsson, Macrocrack Formation in Plasma-Sprayed YSZ TBCs When Spraying Thick Passes, *High Temp. Mater. Processes*, 2005, **9**(3), p 401-413
22. H.B. Guo, R. Vassen, and D. Stover, Atmospheric Plasma Sprayed Thick Thermal Barrier Coatings with High Segmentation Crack Density, *Surf. Coat. Technol.*, 2004, **186**(3), p 353-363
23. J. Matejcek and S. Sampath, In Situ Measurement of Residual Stresses and Elastic Moduli in Thermal Sprayed Coatings – Part 1: Apparatus and Analysis, *Acta Mater.*, 2003, **51**(3), p 863-872
24. J. Matejcek, S. Sampath, D. Gilmore, and R. Neiser, In Situ Measurement of Residual Stresses and Elastic Moduli in Thermal Sprayed Coatings – Part 2: Processing Effects on Properties of Mo Coatings, *Acta Mater.*, 2003, **51**(3), p 873-885
25. S. Sampath and J. Matejcek, "Method and Apparatus for Determining Process-Induced Stresses and Elastic Modulus of Coatings by In Situ Measurement," U.S. Patent 6,478,875, 2002
26. S. Kuroda, T. Fukushima, and S. Kitahara, Simultaneous Measurement of Coating Thickness and Deposition Stress During Thermal Spraying, *Thin Solid Films*, 1988, **164**, p 157-163
27. T. Nakamura and Y. Liu, Determination of Nonlinear Properties of Thermal Sprayed Ceramic Coatings Via Inverse Analysis, *Int. J. Solids Struct.*, 2007, **44**(6), p 1990-2009



28. Y. Liu, T. Nakamura, V. Srinivasan, A. Vaidya, A. Gouldstone, and S. Sampath, Non-Linear Elastic Properties of Plasma-Sprayed Zirconia Coatings and Associated Relationships with Processing Conditions, *Acta Mater.*, 2007, **55**(14), p 4667-4678
29. A. Vaidya, V. Srinivasan, T. Streibl, M. Friis, W. Chi, and S. Sampath, Process Maps for Plasma Spraying of Yttria-Stabilized Zirconia: An Integrated Approach to Design, Optimization and Reliability, *Mater. Sci. Eng. A*, 2008, **497**(1-2), p 239-253
30. T. Streibl, A. Vaidya, M. Friis, V. Srinivasan, and S. Sampath, A Critical Assessment of Particle Temperature Distributions During Plasma Spraying: Experimental Results for YSZ, *Plasma Chem. Plasma Process.*, 2006, **26**(1), p 73-102
31. Y. Liu, T. Nakamura, V. Srinivasan, A. Gouldstone, and S. Sampath, *Optimizing Nonlinear Properties of Thermal Sprayed Coatings Through Processing Parameters* (Boston, MA), Materials Research Society, Warrendale, PA, 2006
32. Y. Liu, T. Nakamura, G. Dwivedi, A. Valarezo, and S. Sampath, Anelastic Behavior of Plasma-Sprayed Zirconia Coatings, *J. Am. Ceram. Soc.*, 2008, **91**, p 4036-4043
33. W. Chi, S. Sampath, and H. Wang, Ambient and High-Temperature Thermal Conductivity of Thermal Sprayed Coatings, *J. Therm. Spray Technol.*, 2006, **15**(4), p 773-778
34. W. Chi, S. Sampath, and H. Wang, Microstructure-Thermal Conductivity Relationships for Plasma-Sprayed Yttria-Stabilized Zirconia Coatings, *J. Am. Ceram. Soc.*, 2008, **91**(8), p 2636-2645
35. A. Vaidya, G. Bancke, S. Sampath, and H. Herman, Influence of Process Variables on the Plasma Sprayed Coatings: An Integrated Study, *International Thermal Spray Conference (ITSC)* (Singapore), ASM International, Materials Park, OH, 2001
36. H. Zhang, H.B. Xiong, L.L. Zheng, A. Vaidya, L. Li, and S. Sampath, Melting Behavior of In-Flight Particles and its Effects on Splat Morphology in Plasma Spraying, *International Mechanical Engineering Congress and Exposition* (New Orleans, LA), ASME, 2002
37. W. Zhang and S. Sampath, A Universal Method for Representation of In-Flight Particle Characteristics in Thermal Spray Processes, *J. Therm. Spray Technol.*, 2008 (accepted)
38. L. Li, A. Vaidya, S. Sampath, H. Xiong, and L. Zheng, Particle Characterization and Splat Formation of Plasma Sprayed Zirconia, *J. Therm. Spray Technol.*, 2006, **15**(1), p 97-105
39. S. Deshpande, A. Kulkarni, S. Sampath, and H. Herman, Application of Image Analysis for Characterization of Porosity in Thermal Spray Coatings and Correlation with Small Angle Neutron Scattering, *Surf. Coat. Technol.*, 2004, **187**(1), p 6-16
40. Z. Wang, A. Kulkarni, S. Deshpande, T. Nakamura, and H. Herman, Effects of Pores and Interfaces on Effective Properties of Plasma Sprayed Zirconia Coatings, *Acta Mater.*, 2003, **51**(18), p 5319-5334
41. A. Kulkarni, Z. Wang, T. Nakamura, S. Sampath, A. Goland, H. Herman, J. Allen, J. Ilavsky, G. Long, J. Frahm, and R.W. Steinbrech, Comprehensive Microstructural Characterization and Predictive Property Modeling of Plasma-Sprayed Zirconia Coatings, *Acta Mater.*, 2003, **51**(9), p 2457-2475
42. A.A. Kulkarni, A. Goland, H. Herman, A.J. Allen, J. Ilavsky, G.G. Long, and F. De Carlo, Advanced Microstructural Characterization of Plasma-Sprayed Zirconia Coatings Over Extended Length Scales, *J. Therm. Spray Technol.*, 2005, **14**(2), p 239-250
43. A. Vaidya, T. Streibl, L. Li, S. Sampath, O. Kovarik, and R. Greenlaw, An Integrated Study of Thermal Spray Process-Structure-Property Correlations: A Case Study for Plasma Sprayed Molybdenum Coatings, *Mater. Sci. Eng. A*, 2005, **403**(1-2), p 191-204